Link to publication

On the fatigue improvement of railways superstructure components due to cold expansion – Part II: Finite element prediction

Giovanni Pio Pucillo[1],*, Alessandro Carrabs[1], Stefano Cuomo[2], Adam Elliott[3], Michele Meo[2]

[1]*Department of Industrial Engineering - University of Naples Federico II, P. le V. Tecchio 80, 80125 Naples, Italy*
[2]*Department of Mechanical Engineering - University of Bath, Claverton Down, Bath BA2 3LT, UK*
[3]*Hird Rail Development Ltd, Clifford House, Lady Bank Drive, Lakeside, Doncaster, DN4 5NF, UK*

Abstract

This paper is the second of a two-part series dealing with the study of the residual stress field induced by cold expansion (CE) in rail-end-bolt holes. In the aeronautical field, cold expansion is a consolidated practice adopted to induce beneficial residual compressive stresses around holes of aluminium parts, with the aim to improve the fatigue strength. However, in the literature few experimental or numerical studies are proposed on the application of this technique to structural steels. In Part I, an in-depth experimental investigation was carried out on railway steel, in particular on rail-end-bolt holes, with the aim to better understand the full non-linear response of the material during the whole process. In this paper, finite element (FE) analyses simulating CE process are presented, and the experimental results of Part I have been used to validate the FE model. The strain-time history acquired during the entire cold expansion process allowed the comparison with FE-predicted strains, both in terms of residual and maximum strains. This approach is not present in literature, neither for aluminium nor for steel. The results, in terms of trend and magnitude, show that strains in both the experiments and the FE simulations are generally consistent, confirming the reliability of the FE model. In addition, a sensitivity study is presented for different levels of cold expansion. The results can be exploited to develop an *a priori* prediction of the residual stresses near the hole surface, aiming to an improvement of fatigue strength.

1. Introduction

Fatigue performance of structural parts is greatly affected by the presence of stress raisers, such as fastener holes, and under tensile dynamic loads these are often the initiation site of fatigue cracks. Cracking is a major issue in the railway field, and in particular at rail-end-bolt holes (Dick 2001; Milo et al. 2018), which causes premature rail replacements, speed restrictions, and a significant impact on rail inspection and maintenance costs (Reid 1993). It is known that fatigue life depends on both material properties (Pucillo et al. 2011) and stress intensity around stress raisers (Carpinteri 1994; Carpinteri, Brighenti, and Spagnoli 2000; Carpinteri, Ronchei, and Vantadori 2013; Brighenti and Carpinteri 2013), and a way to extend lifetime and safety of metal components is the presence of compressive residual stresses around critical points. These stresses have the effect of reducing the actual stress, as well as the stress intensity factor, with a consequent delay of crack initiation and growth.

Cold Expansion (CE) is a common and cost-effective way to induce beneficial compressive residual stresses around fastener holes, and for this reason it has been adopted from the industries for the performance improvement of bolted

---

and riveted joints. The split-sleeve cold expansion process was, in fact, developed by Boing in the late 1960s, and then integrated into a commercial product by Fatigue Technology Incorporated (FTI). Even though the cold expansion process has been mainly used on aircraft structures, thus on aluminium alloys, the flexibility of the process has enabled it to be easily applied also to railway superstructure components, such as mechanical and insulated rail joints (Cannon, Sinclair, and Sharpe 1986; Reid 1993); indeed, based on FTI's Split Sleeve Cold Expansion System, the RailTec System was developed for the rail industry (Fatigue Technology Inc 2016; 2017).

The split-sleeve process is performed by drawing an oversized, tapered mandrel through an internally pre-lubricated split sleeve in the hole (Fig. 1). When the mandrel passes through the hole, the combined major diameter of the mandrel and thickness of the sleeve enlarge the hole, yielding the material directly around the hole and creating the protective zone of residual stresses. This zone protects the hole from the stresses applied to the rail end and significantly decreases the probability of fatigue cracks. The lubricated split sleeve allows for single-side processing, reduces the required pull force, and protects the hole surface from the high frictional forces generated when the mandrel is drawn through the hole. Because of the existence of the split in the sleeve, a small raised pip is formed on the bore of the hole surface. Therefore, the split needs to be aligned with the least critical direction for fatigue crack growth, in order to maximize the benefits of the cold expansion process (Restis and Reid 2002).
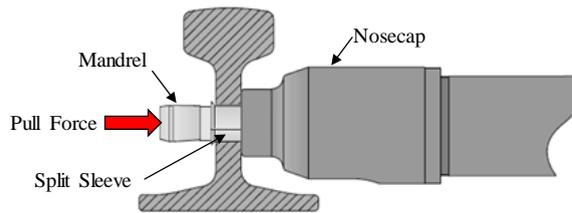

Fig. 1 - Schematic diagram of the FTI RailTec System split sleeve cold working setup.

The fatigue performance improvement is strongly affected by the magnitude and distribution of residual stresses surrounding cold expanded holes, being the total, or effective, stresses the superposition of residual and applied stresses. The knowledge of the residual stress profile is of particular interest in correspondence of critical points of the structure, in case stress intensity factors must be calculated for applying damage tolerance design approach (Carpinteri 1993; Carpinteri, Brighenti, and Vantadori 2006; Aglan and Fateh 2007; Carpinteri and Vantadori 2009; De Iorio, Grasso, Kotsikos, et al. 2012; De Iorio, Grasso, Penta, et al. 2012; Carpinteri, Ronchei, and Vantadori 2013; Grasso et al. 2013; Pucillo, Esposito, and Leonetti 2019a; 2019b).

Investigations on residual stresses in cold expanded holes have been the subject of many research activities, including analytical models, experimental techniques, and numerical simulations. Analytical studies have been performed to determine closed form solutions for residual stresses induced by the cold expansion process. Hsu and Forman (Hsu and Forman 1975) obtained an elastic-plastic solution for residual stresses considering the unloading of the hole after the expansion tool is removed. This solution has been extended to include the effect of reverse yielding during unloading for the plain strain case (Rich and Impellizzeri 1977) and to include the effect of finite size under the plane stress case (Wanlin 1993). However, these solutions are based on two-dimensional approximation (a hole in an infinite sheet (Hsu and Forman 1975) or in a finite circular sheet (Wanlin 1993)) and are unable to predict the through-thickness variation of residual stresses and the geometry domain effect on residual stresses distribution. Many efforts have been made to obtain experimentally the residual stresses by mean of various techniques, as detailed in Part I of this two-part series (Pucillo et al. 2020). However, all of them are affected by some limitations proper of the employed experimental method.

Considering the limitations of analytical solutions and difficulties in measurement of residual stresses by experimental methods and associated limitations, research has focused on developing numerical simulations using the finite element method (FEM) to predict residual stress profiles at cold expanded holes. In the past years, various numerical models have been proposed and used to investigate residual stresses, and two different types of approaches to simulate the cold expansion process have been developed. With the first approach, uniform radial displacements are applied to the hole surface in a single step, simulating the mandrel interference. The recovery of the material is

simulated by removing the applied displacements in a second step. By employing this simple approach, 2-D plane stress/strain, 2-D axisymmetric, and 3-D models have been produced (Priest et al. 1995; Kang, Johnson, and Clark 2002; de Matos et al. 2005; Yongshou et al. 2010; Houghton and Campbell 2012). The second approach is through contact analysis, by modelling the specimen and the mandrel, establishing contact between the hole surface and the mandrel, and making the mandrel to move through the hole, resulting in gradual expansion of the hole and gradual recovery of the material. By employing this complex approach, 2-D axisymmetric and 3-D models have been developed (Chakherlou and Vogwell 2003; Maximov et al. 2009; Yongshou et al. 2010; Houghton and Campbell 2012; Yasniy, Glado, and Iasnii 2017). These simulations have been also extended to include the steel sleeve (de Matos et al. 2004) and the effect of the split in the sleeve (Ismonov et al. 2009). Unfortunately, the proposed models are affected by some limitations: the 2-D plane stress-strain models are unable to predict the through-thickness effects; the 2-D axisymmetric models are unable to simulate realistic boundary conditions; uniform expansion models are limited, because in reality the expansion is applied subsequentially through the axial movement of the mandrel, and are not able to capture the differences in compressive stresses between the entry and the exit faces of the mandrel. However, these last models are useful for a preliminary analysis on the residual stresses of cold expanded holes; contact analysis models between the mandrel and the hole surface are more realistic, but at the same time they require high computational effort.

In the literature few analytical or numerical studies exist on the investigation of residual stresses/strains surrounding cold expanded rail-end-bolt holes (Duncheva and Maximov 2013): many of the above mentioned research activities refer to the application of this technique to aluminium alloys (Hsu and Forman 1975; Wanlin 1993; Priest et al. 1995; Kang, Johnson, and Clark 2002; Chakherlou and Vogwell 2003; de Matos et al. 2004; 2005; Rich and Impellizzeri 1977; Maximov et al. 2009; Ismonov et al. 2009; Yongshou et al. 2010; Houghton and Campbell 2012; Yasniy, Glado, and Iasnii 2017).

Thus, the present work tries to offer a contribution to better understanding the whole stress-strain field surrounding cold expanded steel rail-end-bolt holes, that is not present in the current literature. To reach this goal a uniform expansion approach has been employed to develop the proposed finite element model. Afterwards, the model is validated by means of the experimentally measured strains presented in Part I (Pucillo et al. 2020). The three-dimensional nature of the resulting stress field will be discussed, and differences in stresses as a function of various percentages of cold expansion will be addressed.

The percentage of CE is defined as the magnitude of the normalized radial expansion of the hole during the process and is given by:

$$CE\ [\%] = \frac{R_{mj} + t_s - r_i}{r_i} \times 100$$

where R_{mj} is the mandrel major radius, t_s is the sleeve thickness, and r_i is the initial radius of the hole.

2. Finite Element Modelling

2.1. General configuration and material properties

In the railway industry the cold expansion process is already applied on the holes of railway joints, with the aim to improve their fatigue performances. However, available knowledge (Lindh, Taylor, and Rose 1980) deal with old steels, adopted in the 70s, and in literature there is no data on the steels currently used for railway, such as R260 rail steel. For these reasons, to evaluate the repeatability of the process and considering a scheduled fatigue testing campaign to be performed on specimens to be extracted from drilled rails, a 1.362-meter-long 60E1 rail segment having six holes with a nominal diameter of 32 mm (Fig. 2) was used for the experimental investigation described in Part I (Pucillo et al. 2020). Before the holes were expanded, part of the head and of the foot were removed to create the gripping areas of the specimens that will be extracted from the rail, after having verified that head and foot cutting does not affect the residual stress field around the cold expanded hole (Pucillo 2019).
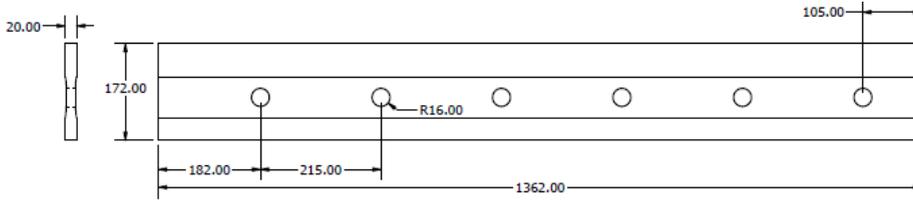
Fig. 2. Component obtained from a drilled rail by removing part of the head and of the foot.

All the simulations were carried out using the Abaqus software version 6.11 (Simulia 2011). The nonlinear R260 nominal (or engineering) stress-strain curve was experimentally measured by the average of five tensile tests. This resulted in a Young's modulus of 210 GPa, a 0.2% offset yield strength of 507 MPa, and a Poisson's ratio of 0.33. Since Abaqus allows the input of pairs of true stress/logarithmic plastic strain coordinates to define the material hardening law, the true stress-plastic strain curve, $\sigma_{true}(\varepsilon^p{}_{ln})$, was obtained (see Fig. 3) from the nominal one, $\sigma_{nom}(\varepsilon_{nom})$, by means of the well-known relationships:

$$\sigma_{true} = \sigma_{nom}(1 + \varepsilon_{nom})$$

$$\varepsilon_{ln} = ln(1 + \varepsilon_{nom})$$

$$\varepsilon^p{}_{ln} = \varepsilon_{ln} - \frac{\sigma_{true}}{E}$$
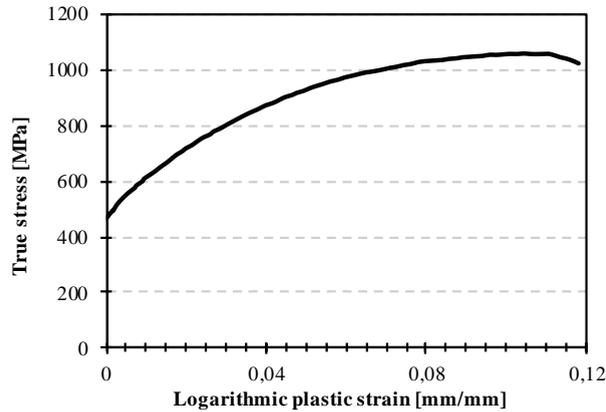

Fig. 3. True stress vs. logarithmic plastic strain curve of the R260 rail steel.

2.2. Geometry and boundary conditions

For the investigation of the effects on the residual stress field due to various percentage of CE, a single-hole 3-D FE model was developed. The interference generated when the mandrel is pulled through the hole was simulated by applying a uniform expansion to the hole. For this purpose, a radial displacement was imposed, and then removed, to the nodes belonging to the hole edge. Being the percentages of simulated CE equal to 1.0%, 2.0%, and 4.0%, the applied radial displacements were, respectively, 0.16 mm, 0.32 mm, and 0.64 mm.

The geometry is a 430 mm long drilled component, and because of the double symmetry with respect to the rail longitudinal and transversal planes, of both geometry and loading conditions, just a quarter of the component was modelled, as shown in Fig. 4. Symmetry boundary constraints were imposed along the Z direction to the nodes belonging to the plane of equation z = 0, and along the X direction to the nodes belonging to the planes of equation x = 0 (Fig. 4-a).

The finite element model is presented in Fig. 4-b. The mesh is composed by 85698 8-node linear brick reduced integration elements (C3D8R) and 2619 6-node linear triangular prism elements (C3D6), the latter adopted for the transition mesh; the total number of nodes is 98600.
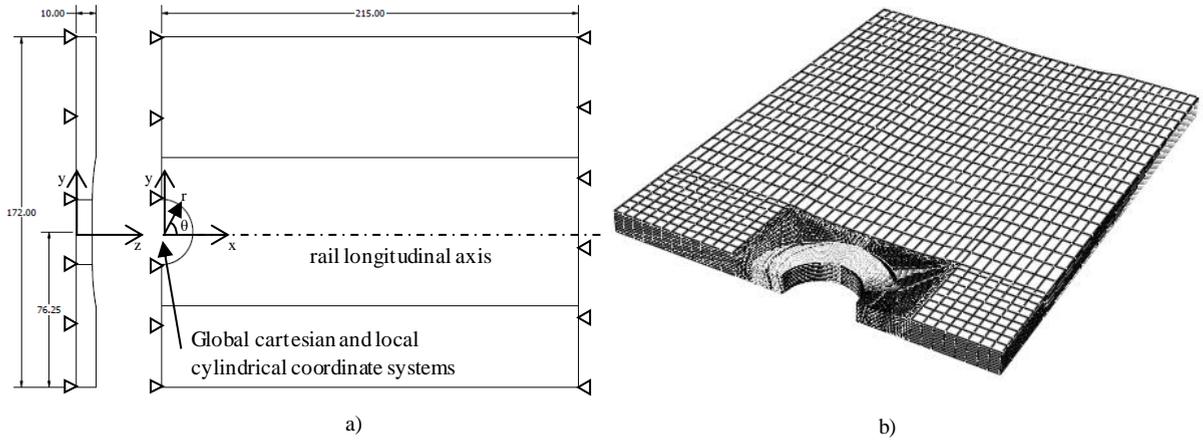

Fig. 4. Geometry and boundary conditions (a), and mesh (b) of the FE model.

3. Results

The effects of cold expansion on the residual stress field arising near the hole are presented in this section. To provide a better understanding of the 3-D nature of the residual stress field, both the hoop and the radial residual stresses are reported. The stresses are expressed in the local cylindrical coordinate system centred on the hole (see Fig. 4-a).

Contour plots of the residual stress fields after CE of 1.0%, 2.0%, and 4.0%, are presented in Fig. 5 and Fig. 6, that refer to the hoop stresses and to the radial stresses, respectively. Fig. 5 clearly shows the through-thickness variation of the hoop residual stress, and that the maximum compressive stresses after cold expansion are observed at the mid-thickness of the rail web for all the percentages of CE. When CE percentage increases from 1.0% to 4.0% the maximum compressive hoop stress increases from 667 MPa to 1027 MPa. Differently, Fig. 6 shows that radial stresses are almost zero on the hole surface (equilibrium condition) and that the maximum compressive values are observed on the surface of the rail web. When CE percentage increases from 1.0% to 4.0% the maximum compressive radial stress increases from 194 MPa to 312 MPa.

Focusing on the hoop stress, which represents the most significant factor affecting the fatigue strength improvement created by CE, the residual stresses distribution on the hole edge, both on the surface and on the mid-thickness of the rail web, was evaluated as a function of the angular coordinate θ (cylindrical coordinate system of Fig. 4-a) and for an increasing percentage of CE. The obtained residual stress profiles are shown in Fig. 7, showing that, as mentioned before, the compressive stresses at the mid-thickness (prefix "*Mid*" in Fig. 7) are higher than the surface (prefix "*Top*" in Fig. 7) of the rail web. As a consequence, the critical area for crack initiation is the rail web surface due to the reduced level of compressive residual stresses induced by the CE.
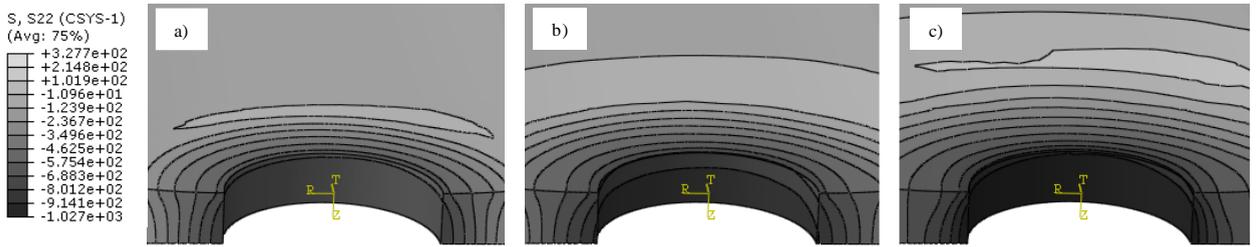
Fig. 5. Contour plot of hoop residual stresses for different percentages of expansion.
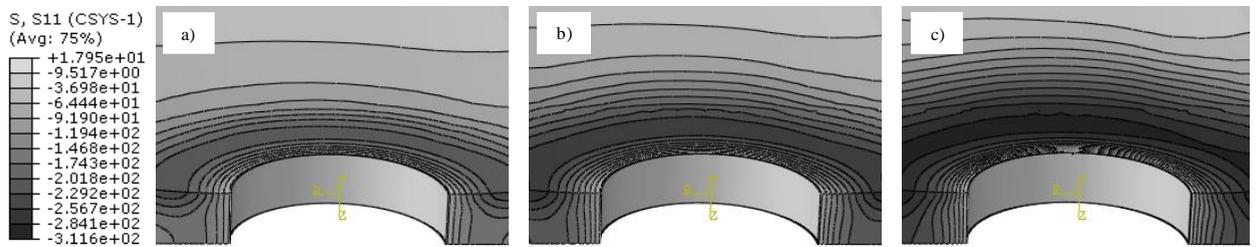

Fig. 6. Contour plot of radial residual stresses for different percentages of expansion.
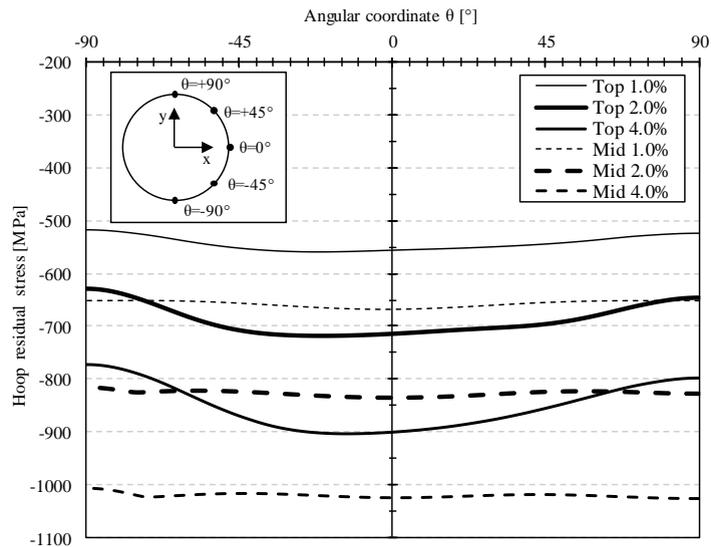

Fig. 7. Hoop residual stresses on the hole edge as a function of the angular coordinate θ and for different percentages of cold expansion. *Top*: rail web surface; *Mid*: mid-thickness of the rail web.

Furthermore, the residual stress filed at the edge of the hole (Fig. 7), for a certain percentage of CE, depends on the angular coordinate θ, in good agreement with literature. As stated in (Lowry 1991; Ball and Lowry 1998), the effectiveness of cold expansion is influenced by the distance between the hole and the edge of the specimen, with lower residual stresses (lower in magnitude) expected for short edge distance. Comparing residual stresses on the rail web surface at $\theta = +90°$, $0°$, $-90°$, it is interesting to observe that the lowest compressive residual stress is obtained at

θ = -90°, because of the shorter edge distance (60.25 mm) compared to that at θ = +90° (79.75 mm) and at θ = 0° (199 mm). At the mid-thickness of the rail web, instead, the stress field is rather uniform compared to the surface.

In rails with not cold expanded holes cracks generally initiate (stress concentration effect due to the hole) from the hedge and propagate along planes lying at ±45° respect to the rail longitudinal axis (Mayville and Stringfellow 1995; Zerbst et al. 2009; Cannon et al. 2003). In these singular points of the railway superstructure high impact forces are induced due to trains motion (Talamini, Jeong, and Gordon 2007; Mandal, Dhanasekar, and Sun 2016; Kerr and Cox 1999), often with amplified effects due to weak ballast conditions (Pucillo et al. 2018; De Iorio et al. 2016). Considering that cold-expansion-induced residual stresses at the hole edge do not assume the maximum intensity at θ = ±45° (Fig. 7), it is reasonable to assume that at cold-expanded holes cracks will initiate and propagate at ±45° as well.

For this reason, and with the aim to develop a LEFM-based model for crack growth prediction (Ball and Lowry 1998; Carpinteri 1993; Carpinteri, Ronchei, and Vantadori 2013) for cold-expanded holes, the knowledge of residual stresses normal to the crack plane (e.g. hoop residual stresses along the direction at θ = ±45°) is essential to determine the residual stress intensity factor K_{res}. For this purpose, the distribution of hoop residual stresses on the rail web surface along the directions at θ = ±45°, as a function of the distance from the hole edge and for an increasing percentage of CE, was evaluated and is shown in Fig. 8; the normalized distance to the hole radius is also shown on the secondary axis. The hoop residual stress assumes the maximum compressive value at the edge of the hole, and gets to the maximum tensile stress with increasing distance from the hole edge. After this point, the tensile stress gradually decreases to zero. When CE percentage increases from 1.0% to 4.0%, the maximum compressive hoop stress increases from 543 to 854 MPa at θ = +45°, and from 551 to 869 MPa at θ = -45°, while maximum tensile stress increases from 95 to 167 MPa along the direction at θ = +45°, and from 109 to 233 MPa along the direction at θ = -45°. The extension of the region of compressive residual stresses also increases with the CE percentage: from 0.83 to 1.56 times the hole radius along the direction at θ = +45°, and from 0.83 to 1.54 times the hole radius along the direction at θ = -45°.
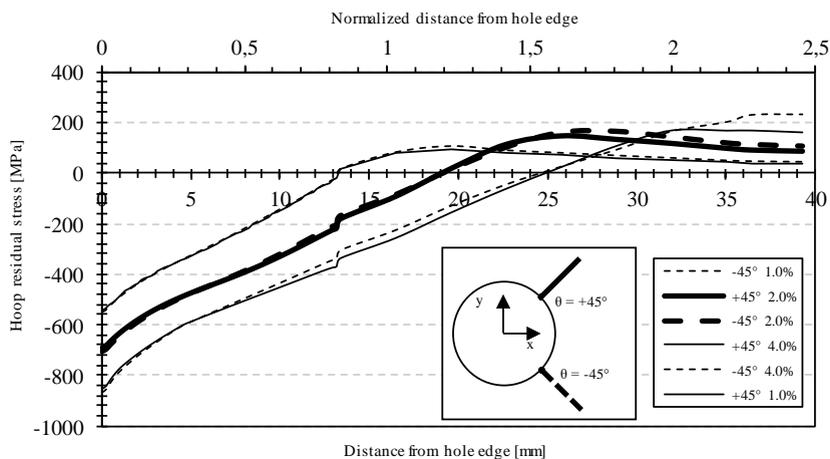

Fig. 8. Hoop residual stress profiles along the direction at θ = ±45° for different percentages of cold expansion.

The radial residual stress profiles are shown in Fig. 9. Stress is almost zero at the hole edge (an equilibrium condition is verified), decreases until to a maximum compressive value, then radial residual stress gradually approaches back to zero. With the increasing CE percentage, the maximum compressive value increases from 195 to 294 MPa along the direction at θ = +45°, and from 183 to 287 MPa along the direction at θ = -45°, and the distance from hole edge corresponding to maximum value increases from 0.59 to 0.82 times the hole radius along the direction at θ = +45°, and from 0.57 to 0.81 times the hole radius along the direction at θ = -45°.
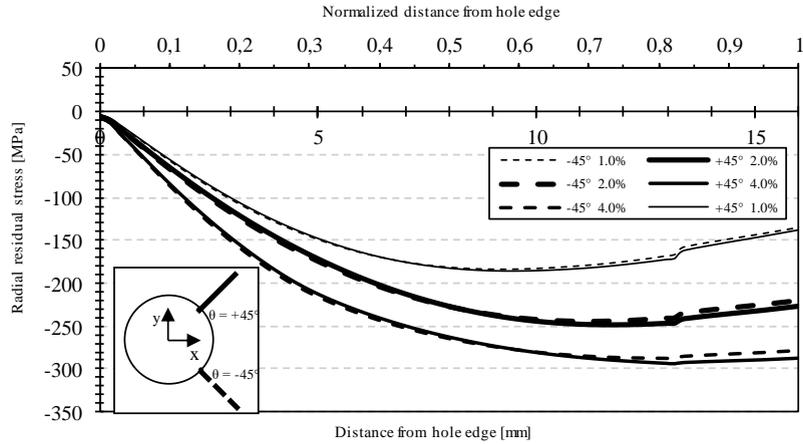
Fig. 9. Radial residual stress profiles along the direction at $\theta = \pm45°$ for different percentages of cold expansion.

For the purpose of validating the single-hole 3-D FE model, the strain distribution surrounding the hole was investigated for the 2.0% CE. In detail, both radial and hoop stresses were evaluated at the end of the stages of hole expansion (maximum strains, because corresponding to the maximum diameter of the hole) and hole recovery (residual strains), along the directions at 0°, ±45°, and ±90° respect to rail longitudinal axis. Predicted maximum and residual strains as a function of the distance from hole edge are shown in Fig. 10 and Fig. 11, respectively.
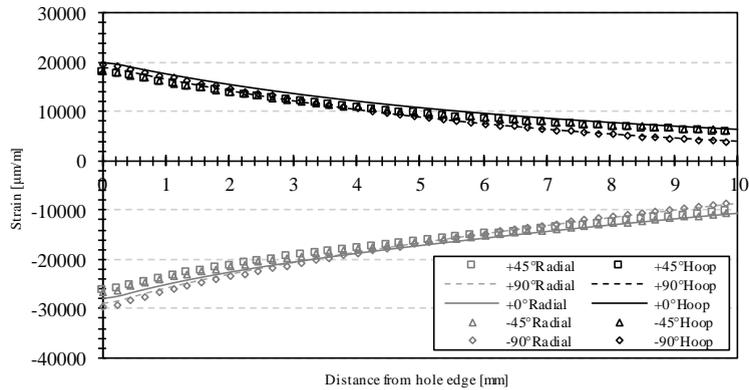

Fig. 10. Maximum strain profiles along the directions at $\theta = 0°$, $\theta = \pm45°$, and $\theta = \pm90°$.

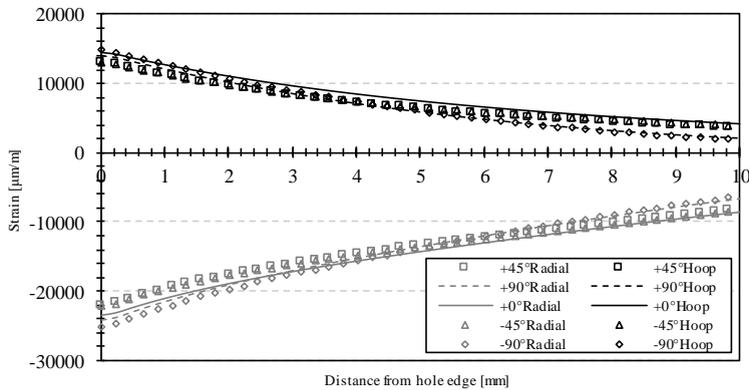Fig. 11. Residual strain profiles along the directions at $\theta = 0°$, $\theta = \pm45°$, and $\theta = \pm90°$.

4. FE model validation

For the validation of the proposed FE model, the comparison between the FE results predicted in the present work and those acquired during the experimental investigations conducted by the authors and illustrated in Part I (Pucillo et al. 2020) is described in this Section.

In the experimental work, the 2.0% cold expansion process application on rail-end-bolt holes was investigated, using both 2D-DIC and strain gauges measurements. The cold expansion process was applied to three rail holes, having an equal nominal diameter and differently equipped with strain gauges mounted on the rail web surface, in particular at the mandrel entry face. In detail, strain gauges were installed in specific angular locations (respect to the reference direction of the cylindrical coordinate system defined in Fig. 4-a) and at specific distances from the hole edge. Considering the strong repeatability of the applied cold expansion process (Pucillo et al. 2020), the results obtained on each hole were considered together, as if all had been acquired during the expansion of a single hole. This allowed to extrapolate the distribution of the hoop strain as a function of the distance from the hole edge along the directions at $\theta = 0°$ and $\theta = +45°$, which are the most interesting ones in terms of residual stress distribution.

Exploiting the installed strain gauges, the strain-time history was acquired during the entire cold expansion process, allowing the comparison between the experimental and FE-predicted strains both in terms of residual and maximum strains. This is not present in the current literature, and guarantees a detailed check of the FE model reliability. It is important to take into account, indeed, that in elasto-plastic analyses it is appropriate to compare both residual and maximum strain values predicted by FEM with those obtained experimentally, since the stress state depends on the loading history of the material (Lee and Barkey 2012).

Fig. 12 shows the comparison between the experimental results and the finite element simulations in terms of hoop residual strains along the directions at $\theta = 0°$, $\pm 45°$, and $\pm 90°$. A very good agreement is observed at $0°$, $+45°$, and $+90°$, both in terms of trend and magnitude, whereas some slight differences can be noted for the directions at $\theta = -45°$, and $\theta = -90°$.
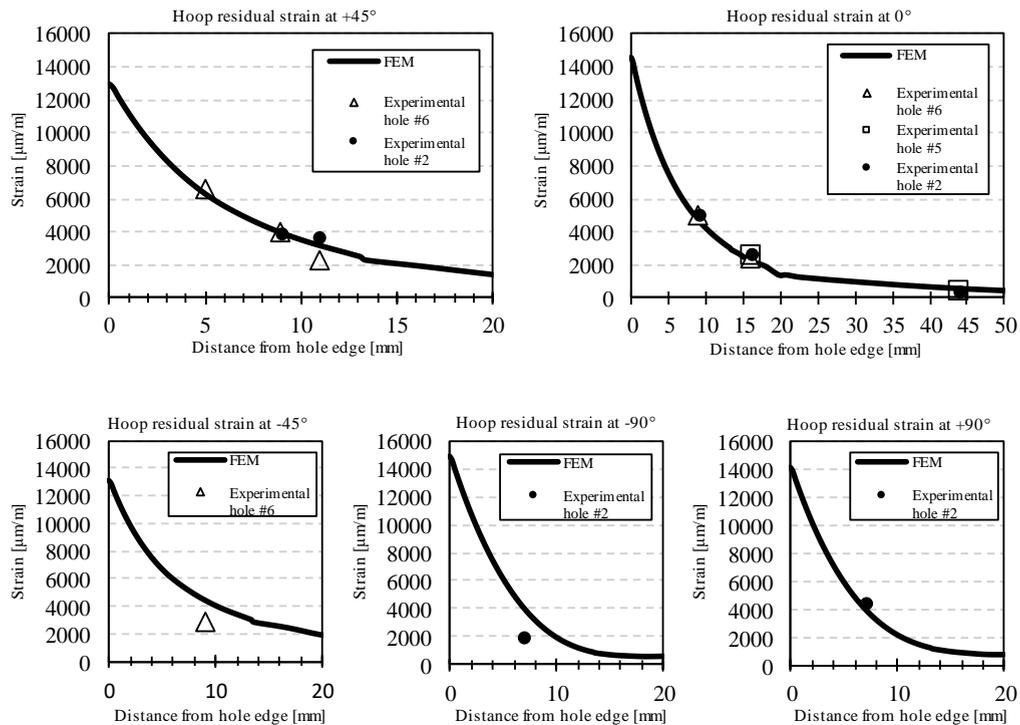

Fig. 12. Comparison of measurement results and simulation results of hoop residual strains along directions at 0°, ±45°, and ±90°.

The comparison between hoop maximum strains measured by strain gauges and by finite element simulation is presented in Fig. 13, where it is found that numerical results agree well with experimental ones.

The comparison between predicted radial strains and measured ones is shown in Fig. 14. Also in this case, a good agreement is observed for both maximum and residual strains.

In summary, it is possible to appreciate a good agreement between the experimental results and the FE predictions; this guarantees the validation of the finite element model proposed in this study, which may be used for the development of an LEFM-based methodology for crack growth prediction at cold-expanded holes.
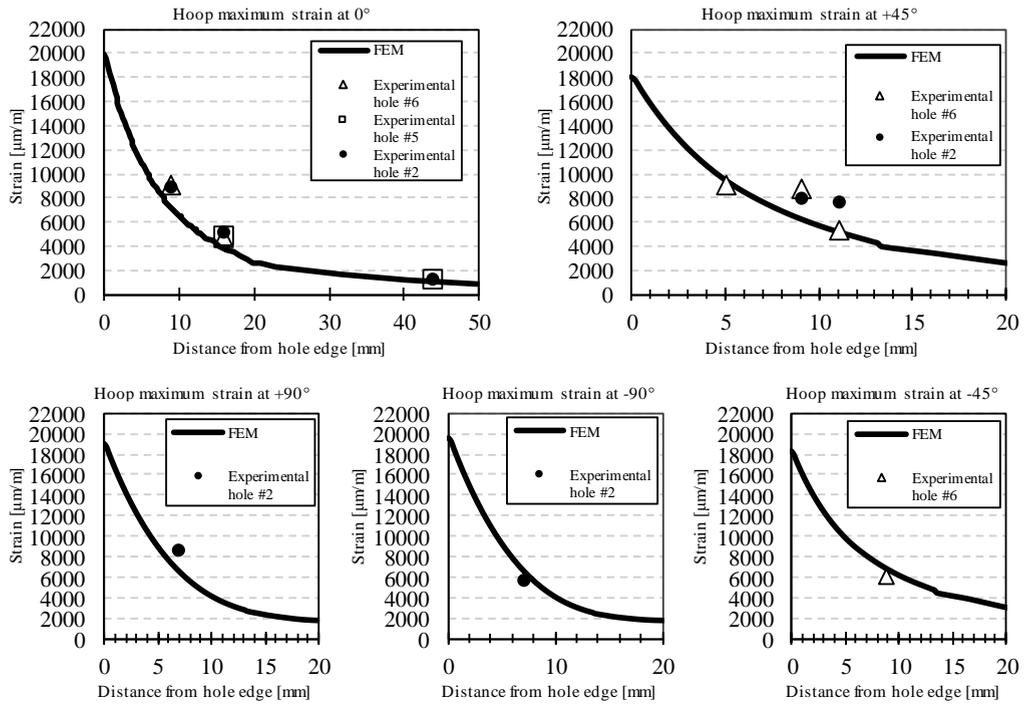

Fig. 13. Comparison of measurement results and simulation results of hoop maximum strains along directions at 0°, ±45°, and ±90°.
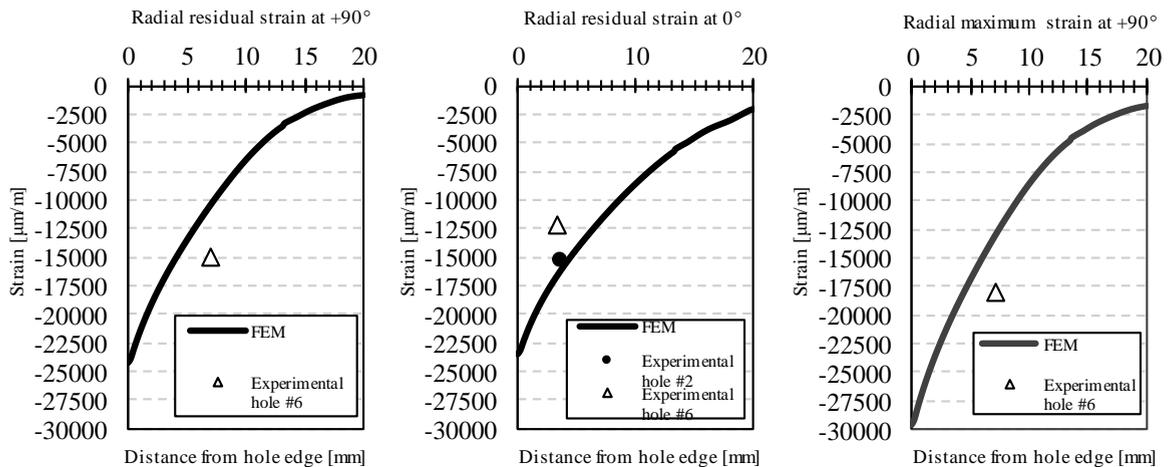

Fig. 14. Comparison of simulation results and measurement results of radial maximum strains along the direction at +90° and of residual strains along directions at +90° and 0°.

5. Conclusions and future works

A simplified 3D FE model has been developed to predict the residual stresses induced by the application of the cold expansion process to rail-end-bolt holes.

The results reveal the three-dimensional and not axisymmetric nature of the residual stress field surrounding the hole. It is found that the distribution and values of residual stresses are significantly affected by the percentage of cold expansion, and significant differences in terms of residual stresses exist through the rail web thickness.

The comparison of the strain gauges results with those calculated by FEM shows a good agreement for both the residual strain field and the one corresponding to the stage of maximum expansion of the hole. This result guarantees the validation of the finite element model, which may be adopted for the development of an LEFM-based model for crack growth prediction at cold-expanded holes.

Future studies will provide for: the development of a 3-D FE model that simulates the interaction between the mandrel-sleeve assembly and the hole surface for a more in-depth investigation of the residual stress field along the thickness of the rail hole; the simulation of hole drilling and, successively, of cold expansion, once the residual stresses due to the manufacturing process of the rail is known and used as initial input (initial state) in the FE model, in order to predict the effective stresses acting at cold expanded rail-end-bolt holes.

Acknowledgements

References

Aglan, H.A., Fateh, M., 2007. Fracture and Fatigue Crack Growth Analysis of Rail Steel. Journal of Mechanics of Materials and Structures 2 (2), 335–346.

Ball, D.L., Lowry, D.R., 1998. Experimental Investigation on the Effects of Cold Expansion of Fastener Holes. Fatigue and Fracture of Engineering Materials and Structures 21 (1), 17–34.

Brighenti, R., Carpinteri, A., 2013. Surface Cracks in Fatigued Structural Components: A Review. Fatigue & Fracture of Engineering Materials & Structures 36, 1209–1222.

Cannon, D.F., Edel, K.-O., Grassie, S.L., Sawley, K., 2003. Rail Defects: An Overview. Fatigue & Fracture of Engineering Materials & Structures 26 (10), 865–886.

Cannon, D.F., Sinclair, J., and Sharpe, K.A., 1986. Improving the fatigue performance of bolt holes in railway rails by cold expansion, International Conference and Exposition on Fatigue, Corrosion Cracking, Fracture Mechanics and Failure Analysis. Salt Lake City, Utah, USA, 353–369.

Carpinteri, A., Vantadori, S., 2009. Sickle-Shaped Surface Crack in a Notched Round Bar under Cyclic Tension and Bending. Fatigue & Fracture of Engineering Materials & Structures 32 (3), 223–232.

Carpinteri, A., 1994. "*Handbook of Fatigue Crack Propagation in Metallic Structures - Volume 2*". Carpinteri, A. (Ed.), Elsevier, Amsterdam, pp. 834.

Carpinteri, A., 1993. Shape Change of Surface Cracks in Round Bars under Cyclic Axial Loading. International Journal of Fatigue 15 (1), 21–26.

Carpinteri, A., Brighenti, R., Spagnoli, A., 2000. External Surface Cracks in Shells under Cyclic Internal Pressure. Fatigue & Fracture of Engineering Materials and Structures 23 (6), 467–476.

Carpinteri, A., Brighenti, R., Vantadori, S., 2006. Surface Cracks in Notched Round Bars under Cyclic Tension and Bending. International Journal of Fatigue 28 (3), 251–260.

Carpinteri, A., Ronchei, C., Vantadori, S., 2013. Stress Intensity Factors and Fatigue Growth of Surface Cracks in Notched Shells and Round Bars: Two Decades of Research Work. Fatigue & Fracture of Engineering Materials & Structures 36 (11), 1164–1177.

Chakherlou, T.N., Vogwell, J., 2003. The Effect of Cold Expansion on Improving the Fatigue Life of Fastener Holes. Engineering Failure Analysis 10 (1), 13–24.

De Iorio, A., Grasso, M., Penta, F., Pucillo, G.P., 2012. A Three-Parameter Model for Fatigue Crack Growth Data Analysis. Frattura ed Integrità Strutturale 21, 21–29.

De Iorio, A., Pucillo, G.P., De Vita, G., Musella, S., Rossi, S., Testa, M., Leonetti, D., 2016. The Reliability of the Locking Devices of the Switches. Role of the Ballast Bed. International Review on Modelling and Simulations 9 (6), 473–478.

De Iorio, A., Grasso, M., Kotsikos, G., Penta, F., Pucillo, G.P., 2012. Development of Predictive Models for Fatigue Crack Growth in Rails. Key Engineering Materials 488–489, 13–16.

de Matos, P.F.P., Moreira, P.M.G.P., Camanho, P.P., de Castro, P.M.S.T., 2005. Numerical Simulation of Cold Working of Rivet Holes. Finite Elements in Analysis and Design 41 (9-10), 989–1007.

de Matos, P.F.P., Moreira, P.M.G.P., Pina, J.C.P., Dias, A.M., de Castro, P.M.S.T., 2004. Residual Stress Effect on Fatigue Striation Spacing in a Cold-Worked Rivet Hole. Theoretical and Applied Fracture Mechanics 42 (2), 139–148.

Dick, C.T., 2001. "*Factors Affecting the Frequency and Location of Broken Railway Rails and Broken Rail Derailments*". University of Illinois at Urbana-Champaign (Ed.), Urbana, IL, USA pp. 268.

Duncheva, G.V., Maximov, J.T., 2013. A new approach to enhancement of fatigue life of rail-end-bolt holes. Engineering Failure Analysis 29, 167–179.

Fatigue Technology Inc., 2016. RailTecTM System, FTI Process Specification 2009-03 Revision E.

Fatigue Technology Inc., 2017. FTI Process Specification 8101 Revision K.

Grasso, M., Penta, F., Pinto, P., Pucillo, G.P., 2013. A Four-Parameters Model for Fatigue Crack Growth Data Analysis. Frattura ed Integrità Strutturale 26, 69–79.

Houghton, S.J., and Campbell, S.K., 2012. Identifying the residual stress field developed by hole cold expansion using finite element analysis. Fatigue and Fracture of Engineering Materials and Structures 35 (1), 74–83.

Hsu, Y.C., Forman, R.G., 1975. Elastic-plastic analysis of an infinite sheet having a circular hole under pressure. Journal of Applied Mechanics 42 (2), 347–352.

Ismonov, S., Daniewicz, S.R., Newman, J.C., Hill, M.R., Urban, M.R., 2009. Three dimensional finite element analysis of a split-sleeve cold expansion process. Journal of Engineering Materials and Technology 131 (3), paper #031007.

Kang, J., Johnson, W.S., Clark, D.A., 2002. Three-dimensional finite element analysis of the cold expansion of fastener holes in two aluminum alloys. Journal of Engineering Materials and Technology 124 (2), 140–145.

Kerr, A.D., Cox, J.E., 1999. Analysis and Tests of Boned Insulted Rail Joints Subjected to Vertical Wheel Loads. International Journal of Mechanical Sciences 41 (10), 1253–1272.

Lee, Y., Barkey, M.E., 2012. Fundamentals of Cyclic Plasticity Theories, in: "*Metal Fatigue Analysis Handbook*". In: Lee, Y., Barkey, M.E., Kang, H. (Ed.). Butterworth-Heinemann, Walthman, MA, USA, pp. 632.

Lindh, D.V., Taylor, R.Q., Rose, D.M., 1980. Sleeve Expansion of Bolt Holes in Railroad Rail. US Federal Railroad Administration, Office of Research and Development.

Lowry, D.R., 1991. D6ac Steel Bolt Hole Life Improvement, F-111 Coldwork Modification Development Program (Phase II), Tech. Rep. FZS-12.

Mandal, N.K., Dhanasekar, M., Sun, Y.Q., 2016. Impact Forces at Dipped Rail Joints. Proceedings of the Institution of Mechanical Engineers, Part F: Journal of Rail and Rapid Transit 230 (1), 271–282.

Maximov, J.T., Duncheva, G.V., Ganev, N., and Bakalova, T.N., 2009. The benefit from an adequate finite element simulation of the cold hole expansion process. Engineering Failure Analysis 16 (1), 503–511.

Mayville, R.A., Stringfellow, R.G., 1995. Numerical Analysis of a Railroad Bolt Hole Fracture Problem. Theoretical and Applied Fracture Mechanics 24 (1), 1–12.

Milo, D., Principe, L., Deng, J., Zhou, K., Liu, X., 2018. A Literature Review of Rail Defect Causal Factors, 2018 ASME Joint Rail Conference, JRC 2018. Pittsburgh, Pennsylvania, USA, paper #JRC2018-6162.

Priest, M., Poussard, C.G., Pavier, M.J., Smith, D.J., 1995. An assessment of residual-stress measurements around cold-worked holes. Experimental Mechanics 35 (4), 361–366.

Pucillo, G.P., Grasso, M., Penta, F., Pinto, P., 2011. On the Mechanical Characterization of Materials by Arcan-Type Specimens. Engineering Fracture Mechanics 78 (8), 1729–1241.

Pucillo, G.P., 2019. Study and Modelling of the Cold Expansion Technique for Holes of the Railway Superstructure - Definition of the Reference Numerical Model and Determination of the Experimental Characteristic Curve [Studio e Modellizzazione della Tecnica di Espansione a Freddo per Fori nell'Armamento Ferroviario], REPORT LS-P0117, Department of Industrial Engineering, University of Naples Federico II, Oct. 2019.

Pucillo, G.P., Carrabs, A., Cuomo, S., Elliot, A., Meo, M., 2020. On the Fatigue Improvement of Railways Superstructure Components Due to Cold Expansion – Part I: Experimental Analysis. Procedia Structural Integrity 28 (C), 1998–2012.

Pucillo, G.P., Esposito, L., Leonetti, D., 2019a. Boundary Conditions Effects on the Crack Growth Mechanism Under Cycling Bending, 2019 ASME Joint Rail Conference, JRC 2019. Snowbird, Utah, USA, paper #JRC2019-1274.

Pucillo, G.P., Esposito, L., Leonetti, D., 2019b. On the Effects of Unilateral Boundary Conditions on the Crack Growth Rate under Cycling Bending Loads. International Journal of Fatigue 124, 245–252.

Pucillo, G.P., De Iorio, A., Rossi, S., Testa, M., 2018. On the Effects of the USP on the Lateral Resistance of Ballasted Railway Tracks, 2018 ASME Joint Rail Conference, JRC 2018. Pittsburgh, Pennsylvania, USA, paper #JRC2018-6204.

Reid, L., 1993. Beneficial Residual Stresses at Bolt Holes by Cold Expansion. Rail Quality and Maintenance for Modern Railway Operation, 337–347.

Restis, J., Reid, L., 2002. FTI Process Specification 8101D: Cold Expansion of Holes Using the Standard Split Sleeve System and Countersink Cold Expansion, Fatigue Technology Inc., Andover Park West, Seattle (WA), USA.

Rich, D.L., Impellizzeri, L.F., 1977. Fatigue Analysis of Cold-Worked and Interference Fit Fastener Holes, in: "*Cyclic Stress-Strain and Plastic Deformation Aspects of Fatigue Crack Growth ASTM STP 637*". In: Impellizzeri, L.F. (Ed.). ASTM, West Conshohocken, PA, pp. 223.

Simulia, Dassault Systèmes, 2011. "*Abaqus 6.11 Theory Manual*" Providence, RI, USA.

Talamini, B., Jeong, D.Y., Gordon, J., 2007. Estimation of the Fatigue Life of Railroad Joint Bars, ASME/IEEE 2007 Joint Rail Conference and Internal Combustion Engine Division Spring Technical Conference. Pueblo, Colorado, USA, paper #JRC/ICE2007-40065.

Wanlin, G., 1993. Elastic-plastic analysis of a finite sheet with a cold-worked hole. Engineering Fracture Mechanics 46 (3), 465–472.

Yasniy, P., Glado, S., Iasnii, V., 2017. Lifetime of aircraft alloy plates with cold expanded holes. International Journal of Fatigue 104, 112–119.

Yongshou, L., Xiaojun, S., Jun, L., Zhufeng, Y., 2010. Finite element method and experimental investigation on the residual stress fields and fatigue performance of cold expansion hole. Materials and Design 31 (3), 1208–1215.

Zerbst, U., Lundén, R., Edel, K. -O., Smith, R.A., 2009. Introduction to the Damage Tolerance Behaviour of Railway Rails – a Review. Engineering Fracture Mechanics 76 (17), 2563–2601.